

$K \rightarrow \pi\nu\bar{\nu}$ spectra and NA62 interpretation

Martin Gorbahn^a, Ulserik Moldanazarova^{a,b}, Kai Henryk Sieja^c, Emmanuel Stamou^c, Mustafa Tabet^c

^a*Department of Mathematical Sciences, University of Liverpool, Liverpool L69 3BX, UK*

^b*Faculty of Physics and Technology, Karaganda Buketov University, 100028 Karaganda, Kazakhstan*

^c*Fakultät für Physik, TU Dortmund, D-44221 Dortmund, Germany*

Using the measured and projected invisible mass spectrum of the $K^+ \rightarrow \pi^+\nu\bar{\nu}$ mode, we determine the current and future constraints within the model-independent framework of the weak effective theory at dimension-six. We work in two different operator bases depending whether neutrinos are Majorana or Dirac fermions. This makes it possible to transparently incorporate mass effects of additional sterile neutrinos for all operators.

1 Introduction

The branching ratio of $K^+ \rightarrow \pi^+\nu\bar{\nu}$ is currently being measured at $\mathcal{O}(35\%)$ accuracy at the NA62 experiment^{1,2} while an accuracy of $\mathcal{O}(15\%)$ is possible to be reached at the end of the runtime. With planned and future experiments like HIKE on the table an accuracy as low as $\mathcal{O}(5\%)$ is expected. In order to quantify the New Physics (NP) sensitivity, this has to be compared with theoretical predictions. In the Standard Model (SM) the decay $K^+ \rightarrow \pi^+\nu\bar{\nu}$ is highly suppressed as it is generated at the loop-level. The total theoretical uncertainty on the SM prediction is $\approx 6\%$ and is dominated by the CKM input parameters, and thus, the rare decay $K^+ \rightarrow \pi^+\nu\bar{\nu}$ has a high sensitivity to NP.

In anticipation of this new data, we consider NP effects to all relevant weak effective theory operators up to dimension-six for both Majorana and Dirac neutrinos including the effect of additional massive sterile neutrinos on the missing-mass spectrum of $K^+ \rightarrow \pi^+\nu\bar{\nu}$. We work in two distinct operator bases depending whether neutrinos are Majorana or Dirac fermions. This allows for a transparent interpretation of possible NP signals in terms of lepton-number violating or lepton-number conserving NP. In order to determine the constraints on the relevant operators, we perform a statistical analysis in a fully frequentist manner and incorporate the full experimental information on the missing-mass distribution.

2 Model Setup

In this section we present the operators bases for the two limiting cases of Majorana and Dirac neutrinos, respectively.

2.1 Majorana- ν EFT

The effective Lagrangian for the $d_i \rightarrow d_j \nu \nu$ transition and Majorana neutrinos at dimension-six reads

$$\mathcal{L}_{d_i \rightarrow d_j \nu \nu}^{(6)} \Big|_{\text{Majorana}} = \sum_{I=\{V,A\}, \tau=\{L,R\}} \sum_f C_f^{I,\tau} O_f^{I,\tau} + \left(\sum_{I=\{S,P,T\}} \sum_f C_f^{I,L} O_f^{I,L} + \text{h.c.} \right), \quad (1)$$

with the interaction type $I = \{V, A, S, P, T\}$ for vector, axial-vector, scalar, pseudoscalar, and tensor, respectively, the chirality $\tau = L, R$ of the fermions with flavour f , and the independent operators

$$O_{abij}^{V,L} = \frac{1}{2} (\bar{\nu}_{Ma} \gamma_\mu \nu_{Mb}) (\bar{d}_i \gamma^\mu P_L d_j), \quad O_{abij}^{V,R} = \frac{1}{2} (\bar{\nu}_{Ma} \gamma_\mu \nu_{Mb}) (\bar{d}_i \gamma^\mu P_R d_j), \quad (2)$$

$$O_{abij}^{A,L} = \frac{1}{2} (\bar{\nu}_{Ma} \gamma_\mu \gamma_5 \nu_{Mb}) (\bar{d}_i \gamma^\mu P_L d_j), \quad O_{abij}^{A,R} = \frac{1}{2} (\bar{\nu}_{Ma} \gamma_\mu \gamma_5 \nu_{Mb}) (\bar{d}_i \gamma^\mu P_R d_j), \quad (3)$$

$$O_{abij}^{S,L} = \frac{1}{2} (\bar{\nu}_{Ma} \nu_{Mb}) (\bar{d}_i P_L d_j), \quad O_{abij}^{P,L} = \frac{1}{2} (\bar{\nu}_{Ma} i \gamma_5 \nu_{Mb}) (\bar{d}_i P_L d_j), \quad (4)$$

$$O_{abij}^{T,L} = \frac{1}{2} (\bar{\nu}_{Ma} \sigma_{\mu\nu} \nu_{Mb}) (\bar{d}_i \sigma^{\mu\nu} P_L d_j). \quad (5)$$

The corresponding Wilson coefficients $C_f^{V/A, L/R}$ of the operators $O^{V/A, L/R}$ further fulfil the condition

$$C_{abij}^{V/A, L/R} = \left(C_{baji}^{V/A, L/R} \right)^*, \quad (6)$$

to ensure the hermiticity of the Lagrangian in Eq. (1). Note that further

$$C_{abij}^{I,\tau} = \eta C_{baji}^{I,\tau} \quad \text{where} \quad \eta = \begin{cases} +1, & \text{for } I = A, S, P \\ -1, & \text{for } I = V, T, \end{cases} \quad (7)$$

due to the Majorana nature of the neutrinos. Altogether this amounts to a total number of 48 independent Wilson coefficients contributing to the $s \rightarrow d \nu \nu$ transition in the case of three Majorana neutrinos.

2.2 Dirac- ν EFT

The effective Lagrangian for the $d_i \rightarrow d_j \nu \bar{\nu}$ transition and Dirac neutrinos at dimension-six reads

$$\mathcal{L}_{d_i \rightarrow d_j \nu \bar{\nu}}^{(6)} \Big|_{\text{Dirac}} = \sum_{\tau, \tau'=\{L,R\}} \sum_f C_f^{V,\tau\tau'} O_f^{V,\tau\tau'} + \sum_f \left(C_f^{S,LL} O_f^{S,LL} + C_f^{S,LR} O_f^{S,LR} + C_f^{T,LL} O_f^{T,LL} + \text{h.c.} \right), \quad (8)$$

with the chiralities $\tau, \tau' = \{L, R\}$ of the neutrino and quark flavours denoted collectively by f . The independent operators in the Lagrangian in Eq. (8) read

$$O_{abij}^{V,LL} = (\bar{\nu}_{Da} \gamma_\mu P_L \nu_{Db}) (\bar{d}_i \gamma^\mu P_L d_j), \quad O_{abij}^{V,LR} = (\bar{\nu}_{Da} \gamma_\mu P_L \nu_{Db}) (\bar{d}_i \gamma^\mu P_R d_j), \quad (9)$$

$$O_{abij}^{V,RL} = (\bar{\nu}_{Da} \gamma_\mu P_R \nu_{Db}) (\bar{d}_i \gamma^\mu P_L d_j), \quad O_{abij}^{V,RR} = (\bar{\nu}_{Da} \gamma_\mu P_R \nu_{Db}) (\bar{d}_i \gamma^\mu P_R d_j), \quad (10)$$

$$O_{abij}^{S,LL} = (\bar{\nu}_{Da} P_L \nu_{Db}) (\bar{d}_i P_L d_j), \quad O_{abij}^{S,LR} = (\bar{\nu}_{Da} P_L \nu_{Db}) (\bar{d}_i P_R d_j), \quad (11)$$

$$O_{abij}^{T,LL} = (\bar{\nu}_{Da} \sigma_{\mu\nu} P_L \nu_{Db}) (\bar{d}_i \sigma^{\mu\nu} P_L d_j). \quad (12)$$

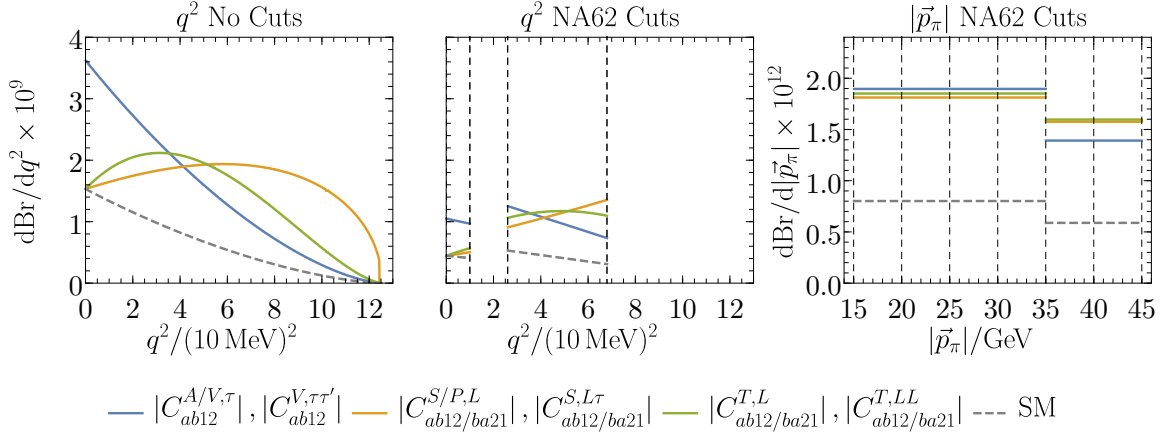


Figure 1 – Differential distributions of $\text{Br}(K \rightarrow \pi \nu \nu)$ for different NP scenarios containing three massless Majorana or Dirac neutrinos, see text for details.

Here the hermiticity condition on the corresponding Wilson coefficients read

$$O_{abij}^{V, \tau \tau'} = \left(O_{baji}^{V, \tau \tau'} \right)^* . \quad (13)$$

Altogether this amounts to a total number of 90 independent Wilson coefficients contributing to the $s \rightarrow d \nu \bar{\nu}$ transition in the case of three Majorana neutrinos.

3 New Physics Sensitivities and Correlations

We first show the differential distributions for the Dirac and Majorana effective theory with three light neutrinos $m_{\nu,1} \approx m_{\nu,2} \approx m_{\nu,3} \approx 0$, and the case of one additional sterile neutrino with mass $m_{\nu,4} = 50 \text{ MeV}$ within the Majorana effective theory with three massless neutrinos. Further, we present the correlations between new diagonal Dirac neutrino couplings and the current and projected limits on the Wilson coefficients for the case of an additional sterile neutrino. Further scenarios can be found in Ref. ³. The limits always correspond to the NP interactions, i.e. in addition to the SM contribution. In case of possible interference terms with the SM, the NP phase is taken to be aligned to the SM phase.

Single-operator fits

Here we only present the limits for the case of a Majorana effective theory with three light neutrinos and an additional sterile neutrino. The Dirac and Majorana scenarios with three massless neutrinos can be found in Ref. ³. Nevertheless, we first show the differential distributions for the Dirac and Majorana case in Fig. 1 and the case of an additional sterile neutrino with mass $m_{\nu,4} = 50 \text{ MeV}$ in Fig. 2 for all independent Wilson coefficients. In both figures the value of the Wilson coefficients are chosen such that they saturate the current experimental limit at 90% CL. As it can be seen in Fig. 1, the case of Majorana and Dirac neutrinos is experimentally indistinguishable.

In the left panel of both figures, we show the differential distribution $\text{dBr}(K^+ \rightarrow \pi^+ \nu \nu)/\text{d}q^2$ while in the middle panels, we show the same but integrated over the pion-momentum signal region of NA62. The right panels show the distributions differential in the pion momentum $|\vec{p}_\pi|$ in the NA62 lab frame integrated over the q^2 signal region of NA62. As it can be seen in both figures, a binning in the missing-momentum squared q^2 is able to distinguish between the different interaction structures but not between the Majorana or Dirac nature of the neutrinos compared to a binning in the pion momentum $|\vec{p}_\pi|$ as currently employed by the NA62 experiment.

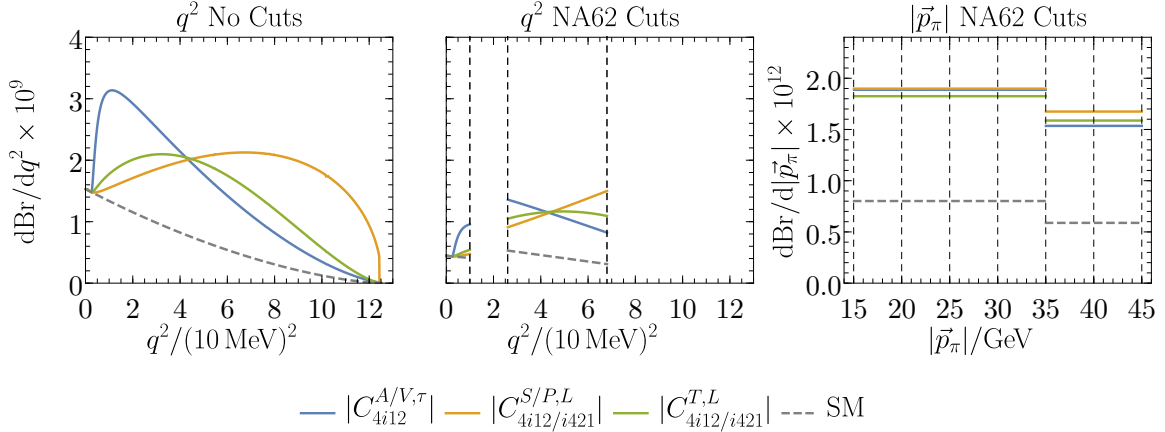


Figure 2 – Differential distributions of $\text{Br}(K \rightarrow \pi \nu \nu)$ for different NP scenarios containing one massive sterile neutrino with mass, $m_{\nu,4} = 50 \text{ MeV}$, see text for details.

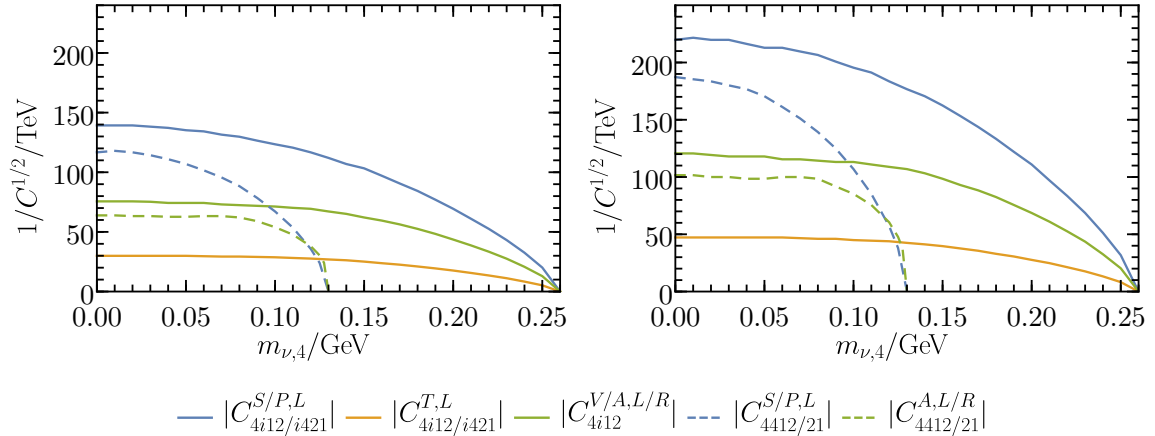


Figure 3 – Current (left) and future (right) lower limits on $1/\sqrt{C}$ at 90% CL for the scenarios with an additional massive sterile neutrino interacting via one of the given NP Wilson coefficients as a function of its mass.

Finally, we show the resulting limits on the Wilson coefficients as a function of the mass of an additional sterile neutrino in Figure 3. In the left panel of Figure 3, we show the current constraints while in the right panel we show the projected ones for the HIKE experiment.

Multi-operator correlations

Here we study the correlation between different NP operators in particular the case of new diagonal Dirac interactions on top of the already present SM contribution. All NP phases are aligned to the SM phase in order to avoid new CP-violating contributions. Additionally, all new interactions are taken to be flavour universal and are switched on at the same time, i.e. $C_{1112}^{V,LL} = C_{2212}^{V,LL} = C_{3312}^{V,LL}$. The results are shown in Fig. 4 where the dark and light blue regions correspond to the allowed regions at 68% and 90% CL. The dashed black line corresponds to the projected expected limit at 90% CL at HIKE assuming a SM like measurement.

4 Conclusion

The rare decay mode $K \rightarrow \pi \nu \nu$ currently probes NP scales up to $\mathcal{O}(100 \text{ TeV})$ and with upcoming and planned experiments the constraints are expected to reach scales as high as $\mathcal{O}(300 \text{ TeV})$. Furthermore, all independent operators contributing to the $q_i \rightarrow q_j \nu \nu$ ($i \neq j$) transition have

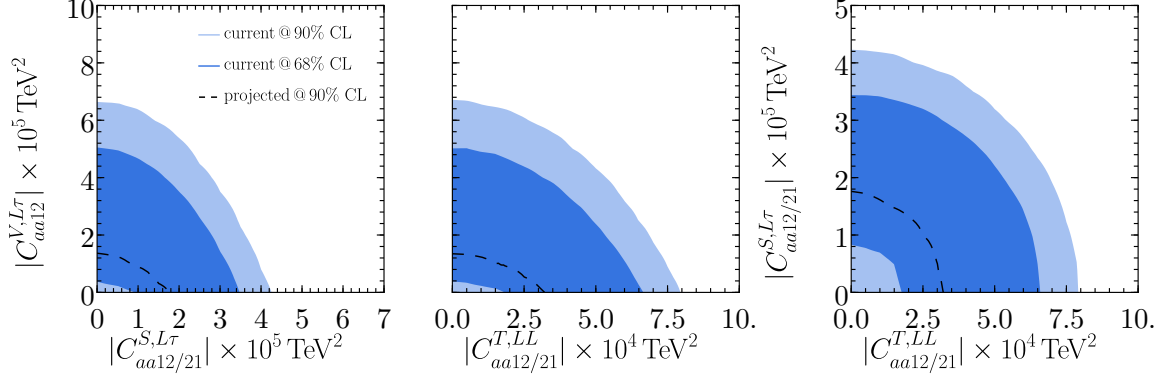


Figure 4 – Allowed parameter space at 68% CL (dark blue) and 90% CL (light blue) in the plane of two NP Wilson coefficients, see text for details.

been classified. While here we only have shown the constraints exemplary for the case of new diagonal flavour universal Dirac interactions, the sensitivities of all independent operators and correlations between them can be found in Ref. ³. There, the expected constraints on the NP scale range from $\mathcal{O}(40 \text{ TeV})$ for tensor operators to $\mathcal{O}(300 \text{ TeV})$ for axial-vector Majorana and the here analysed vector Dirac operators. We further analysed the effect of an additional massive sterile neutrino on the distributions and determined the current and future experimental sensitivity on constraining the corresponding Wilson coefficients as a function of the sterile neutrino mass.

Acknowledgments

This contribution to the EW session of the 58th Rencontres de Moriond 2024 is based on Ref. ³.

References

1. E. Cortina Gil *et al.* [NA62], JHEP **11**, 042 (2020) doi:10.1007/JHEP11(2020)042 [arXiv:2007.08218 [hep-ex]].
2. E. Cortina Gil *et al.* [NA62], JHEP **06**, 093 (2021) doi:10.1007/JHEP06(2021)093 [arXiv:2103.15389 [hep-ex]].
3. M. Gorbahn, U. Moldanazarova, K. H. Sieja, E. Stamou and M. Tabet, [arXiv:2312.06494 [hep-ph]].